

Mesospheric Carbon Dioxide Content As Determined from the CRISTA-1 Experimental Data

V. S. Kostsov and Yu. M. Timofeyev

Research Institute of Physics, St. Petersburg State University, Ul'yanovskaya ul. 1, Petrodvorets, 198504 Russia
e-mail: vlad@troll.phys.spbu.ru; tim@troll.phys.spbu.ru

Received February 14, 2002; in final form, August 28, 2002

Abstract—The paper presents the profiles of mesospheric carbon dioxide content determined in the height range 60–90 km from the outgoing limb radiation measured in November 1994 with the CRISTA satellite instrument in the CO₂ 15- μ m band. The satellite data are interpreted by a combined method with allowance for the effect of nonlocal thermodynamic equilibrium. This method lies in simultaneously retrieving the profiles for the kinetic temperature, pressure, carbon dioxide content, and vibrational temperatures of the lower vibrational states of the four most abundant isotopic modifications of CO₂ molecules. The carbon dioxide mesospheric vertical profiles are analyzed on the basis of about 300 atmospheric scans (all radiation spectra measured in the range from the minimum to the maximum tangent height) measured over the latitude belt 50° S–65° N. It is shown that a decrease in the carbon dioxide volume mixing ratio with height begins, on the average, at a height of 70–75 km. This height is significantly lower than that predicted from numerical models of the upper atmosphere. However, this result is in complete agreement with the carbon dioxide retrieval data obtained from the CRISTA instrument measurements on the basis of a distinctly different approach, which is based on radiation measurements in the 4.3- μ m band and numerical simulation of the nonequilibrium populations of CO₂ vibrational states. This agreement indicates that our results are highly reliable. However, some events of CO₂ uniform mixing up to a height of about 85 km were also revealed. The mean profiles of the carbon dioxide volume mixing ratio measured for the middle latitudes of both hemispheres differ from each other at a height of 90 km by no more than 40 ppmv. The mean latitude gradients of the CO₂ volume mixing ratio in the middle and upper mesosphere reach 4.8 ppmv per 10°. The CO₂ concentration decreases from southern (spring) toward northern latitudes (fall).

1. INTRODUCTION

Carbon dioxide is an important greenhouse atmospheric gas. Its role in the atmospheric energy balance is especially prominent in the height range from 30 to 120 km. IR radiative cooling in the CO₂ 15- μ m band specifies the radiative balance in the Earth's stratosphere, mesosphere, and lower thermosphere. However, there are few measurements of the CO₂ content in these atmospheric layers, especially compared to those performed near the Earth's surface and in the troposphere. For the last two centuries, a significant increase in the surface CO₂ content (the CO₂ volume mixing ratios in 1800 and 1993 were 280 and 356 ppmv, respectively) has been revealed. It leads to a rise in the stratospheric and mesospheric CO₂ content and, as a consequence, to the cooling of these atmospheric layers [1]. A number of investigators have observed stratospheric and mesospheric temperature trends up to 1° per year [2]. The increase of the stratospheric CO₂ content may promote a rise in the ozone concentration—at least by the Chapman cycle through the change of the stratospheric temperature. Estimations show that a doubling of CO₂ in the undisturbed stratosphere may lead to a maximum decrease in its temperature by 7–10 K at a height of 40 km and to an increase in the O₃ content by 6% [1]. None

of the modern numerical models quantitatively explains the significant temperature trends observed in the upper atmosphere.

It has been suggested over many years that CO₂ is uniformly mixed up to a height of 90–100 km. This conclusion is based on earlier rocket mass-spectrometric measurements of the CO₂ density [3–6] and on theoretical simulations [7–10]. There were few rocket measurements, and they gave only a local information on the CO₂ density.

The development of different satellite measuring methods has made it possible to extend the range of studies of atmospheric composition characteristics [11]. Solar radiation absorption measurements along tangent paths (the occultation method) by using a beam-scanning instrument were first realized for the experiments aboard Spacelab 1 [12] and then were repeated in the course of a number of space experiments with the ATMOS IR-interferometer [13]. The measurements performed aboard Spacelab 1 were the first to determine a rapid decrease in the CO₂ volume mixing ratio beginning at a height of about 75 km.

The measurements of the Earth's limb radiation performed in different rocket and space experiments have allowed a significant extension of the region subject to

CO₂ monitoring. The complexity of revealing the CO₂ content from the atmospheric radiation measured for large tangent heights is due to nonlocal thermodynamic equilibrium (non-LTE) conditions. For example, for the CO₂ 15- and 4.3- μm bands, the non-LTE conditions can start in the range 70–90 km and in the stratosphere, respectively. To determine the CO₂ content from radiation measurements, different kinetic models of the population of CO₂ excited states were employed as additional a priori information. The use of the kinetic models in the algorithms of interpreting satellite measurements of the outgoing radiation allowed unambiguous solutions. However, on the other hand, these solutions depended significantly on the adequacy of the kinetic models, on the accuracy of different constants for the processes of excitation and deexcitation of CO₂ molecules, and on additional information on the atmospheric state.

In [14], on the basis of rocket measurements of the atmospheric radiation, the mean profile of the CO₂ content is computed. It demonstrates that the CO₂ volume mixing ratio is constant up to a height of 90 km and then decreases slowly with height.

To determine the CO₂ content in the upper atmosphere, daytime measurements of the Earth's limb radiation in the CO₂ 4.3- μm band were most often used. This is due to both a high daytime intensity of the outgoing radiation in this absorption band and the availability of well-designed kinetic models of population.

The application of the kinetic model of population to an analysis of the NIMBUS 7 SAMS measurements of radiation in the CO₂ 4.3- μm band has led to the CO₂ volume mixing ratio beginning to decrease at 70 km [15]. Similar measurements with the ISAMS instrument aboard the UARS satellite and their analysis with the use of the kinetic model have refined the CO₂ profile obtained from the SAMS data [16]. In this new model of CO₂, a rapid decrease in the CO₂ volume mixing ratio begins at a height of 80 km. Using this new model and the ISAMS data, the authors of [16] have concluded that the latitudinal and seasonal variations of the CO₂ volume mixing ratio do not exceed 10, 14, 23, and 28% at heights of 85, 90, 95, and 100 km, respectively.

A significant volume of new information on the CO₂ content in the upper atmosphere is obtained from the data on the Earth's limb radiation measured with the CRISTA-1 and CRISTA-2 spectrometers during two *Shuttle* flights in November 1994 and August 1997, respectively [10]. The interpretation of the daytime radiation measurements in the CO₂ 4.3- μm band on the basis of the kinetic model has made it possible to obtain the global and height (60–130 km) distributions of the CO₂ density. The temperature and pressure vertical profiles retrieved from the measurements performed in the CO₂ 15- μm band up to a height of 85 km and the model data on the CO₂ distribution above 85 km have allowed the authors of [10] to obtain CO₂ volume mixing ratios that

deviate from the values corresponding to uniform mixing beginning at heights of 70 to 80 km [10]. An analysis of the global data on the daytime CO₂ content has revealed significant latitudinal and longitudinal variations throughout the mesosphere and lower thermosphere (see [10] for details). The available data on the mesospheric CO₂ content are given in Table 1.

This work presents and analyzes the profiles of the CO₂ densities and volume mixing ratios in the height range 60–90-km obtained from the CRISTA-1 experimental data by a combined method with allowance for non-LTE conditions. Computations are performed for 272 atmospheric scans (a scan is a series of radiation spectra measured in the range from the minimum to the maximum tangent height) over the latitude belt 55° S–65° N. We note that this method [17] allows simultaneous retrieval of the temperature, pressure, and CO₂ content profiles from measurements of the Earth's limb nonequilibrium radiation in the 15- μm band without invoking additional a priori information in the form of kinetic models describing the processes of population of the CO₂ excited states. Therefore, this method is free of the drawbacks inherent in the methods used in [10, 14–16]. Instead of these kinetic models, the inversion algorithm uses rather general a priori information, including information based on the results of computations by the kinetic models for the population of CO₂ excited states. As is shown in [18], such an approach allows the formulation of the inversion algorithm that makes the most use of the results of measuring the Earth's limb radiation, which are determined by the instantaneous atmospheric state [18]. It is important that, unlike the methods given in [10, 14–16], the method developed in [17] can be applied to both daytime and nighttime observation conditions.

2. RETRIEVAL ERRORS IN THE MESOSPHERIC CARBON DIOXIDE CONTENT

Before we proceed to an analysis of the results of CO₂ retrieval, it is necessary to briefly describe the peculiarities of the procedure used for the interpretation of the outgoing radiation in the 15- μm band and to analyze the errors in CO₂ remote measurements.

The radiance at frequency ν and tangent height z_t under non-LTE conditions for vibrational states of molecules of atmospheric gases can be represented as a functional of the vertical profiles of a number of atmospheric parameters:

$$I(\nu, z_t) = A[T_k(z), p(z), n_g(z), T_v^{gs}(z)],$$

where A is the nonlinear operator of the forward problem; z is the vertical coordinate; p is the pressure; g and s are the indices denoting a gas and a vibrational state, respectively; T_k is the kinetic temperature; n is the gas concentration; and T_v is the vibrational temperature. In the case under consideration (the CO₂ 15- μm band, the

Table 1. Mesospheric CO₂ content

No.	Information source	Principal conclusions	References
1	Numerical simulation of the atmospheric composition	CO ₂ is uniformly mixed in the mesosphere	7, 8, 9, 10
2	Rocket mass-spectrometric measurements	CO ₂ is uniformly mixed in the atmosphere up to a height of about 100 km	3, 4, 5, 6
3	Rocket measurements of the Earth's limb radiation	CO ₂ volume mixing ratio is constant up to a height of about 90 km and gradually decreases with height above this level	14
4	Satellite measurements of solar radiation absorption	Measurements are performed during sunrises and sunsets	
	Beam-scanning spectrometer, Spacelab 1	CO ₂ volume mixing ratio decreases rapidly, beginning at a height of 75 km	12
	ATMOS interferometer, Spacelab 3	CO ₂ volume mixing ratio is constant within the layer 70–90 km and decreases rapidly at heights of 90–100 km	13
5	Satellite measurements of the Earth's limb radiation (4.3 μm)	Daytime measurements	
	SAMS	CO ₂ volume mixing ratio decreases rapidly, beginning at a height of 70 km	15
	ISAMS	CO ₂ volume mixing ratio decreases rapidly, beginning at a height of 80 km Seasonal and latitudinal variations in the CO ₂ volume mixing ratio do not exceed the measurement errors	16
	CRISTA-1 and CRISTA-2	CO ₂ volume mixing ratio decreases rapidly within the layer 70–80 km. Significant latitudinal and longitudinal variations in the CO ₂ density are observed	10

spectral range 640–685 cm⁻¹), the unknown parameters are as follows: the kinetic temperature, pressure, CO₂ concentration, and vibrational temperatures of different states for four most abundant isotopic modifications of CO₂ molecules. Thus, the vertical profiles of these parameters should be retrieved from the results of spectral–height measurements of the radiance $I(\nu, z_r)$. A comprehensive description of the method of interpretation of satellite measurements of the outgoing IR limb radiation with allowance for the effect of non-LTE conditions is given in [17]. In [19], the profiles of kinetic temperature in the middle atmosphere that are retrieved from the CRISTA-1 data by the method under consideration are analyzed.

Our analysis of both the spectra and the results of [19] has made it possible to improve the method from the standpoint of including the measurement errors and refining the a priori information. In connection to this, the CO₂ profile up to 60 km was assumed to be known in the course of data processing in this work unlike works [17, 19]. The numerical experiments have shown that a priori information of such a kind increases the accuracy of computation of all parameters. This results from the fact that only two parameters, the kinetic temperature and pressure, are unknown when the combined inverse problem is being solved for the height range from 40 to 60 km. We also note that this refinement of a priori information allows us to somewhat reduce a priori limitations on the smoothness of the volume mix-

ing ratio profile and to use the 20-km correlation distance in the model correlation matrix instead of the 25-km distance used in the earlier versions [17].

The principal sources of errors controlling the accuracy of the inverse problem solution are as follows: random noise (the detector and electronics), inaccuracy of spectral calibration, nonlinearity of absolute calibration, inaccuracy in the tangent height, frequency-scale shift due to mechanical phenomena in the instrument, effect of detector relaxation, uncertainties of the instrument line-shape and angle functions, inaccuracy of the radiative transfer model, and inaccuracies of the numerical implementation of the algorithm.

The random noise was taken into account immediately in the algorithm of inversion of radiation data. The correction of the effect of detector relaxation, the refinement of the instrument line-shape function, and the correction of the nonlinearity of absolute calibration were performed in the course of preprocessing of the measured data. The effect of the uncertainty of the instrument angle function is negligible compared to other sources of errors. The inaccuracy of spectral calibration and the scale shift were corrected in the course of solving the inverse problem. The inaccuracy of determining the tangent height is taken into account in the form of an additional effective random noise of measurements. The comparison of the computer code used by us to determine the nonequilibrium radiation with its analogues used abroad shows that the inaccu-

racy of the numerical implementation of the algorithm has a negligibly small effect on the solution of the inverse problem [20].

On the basis of the above corrections, residual uncertainties were estimated and were also included as an additional effective random noise of measurements. Two exceptions are the nonlinearity of absolute calibration and the inaccuracy of the radiative transfer model, which influence the results in a clearly defined systematic manner, and therefore they were estimated separately. Such an approach allowed the estimation of the random and systematic components of the retrieval error. The former is due to the total effective noise, and the latter is due to both the inaccuracy of the radiative transfer model and the residual uncertainty remaining after correction of the nonlinearity of absolute calibration. In this case, the term “inaccuracy” means the neglect of the effect of non-LTE conditions for the upper vibrational states of CO₂ molecules and for all the states of O₃ molecules.

We emphasize that, in the inversion algorithm, the retrieved parameter describing the CO₂ content is the number concentration (density); the CO₂ volume mixing ratios and their errors were computed from the retrieved values of the temperature, pressure, concentration, and the corresponding errors. The estimates of the systematic and random components of the error in the CO₂ volume mixing ratio profile are rounded off to integers and are given in Table 2. It is seen that the random component does not exceed 11–13 ppmv for the height range up to 85 km and increases up to 17 ppmv at a height of 90 km. Below 80 km, the systematic error component is comparable with the random one, and, above 80 km, it increases substantially and reaches 50 ppmv at a height of 90 km. The relative random error component does not exceed 5% up to a height of about 85 km and is equal to 8% at a height of 90 km, and the relative systematic error component reaches 25% at a height of 90 km. We emphasize that the procedure without consideration of the nonlinearity of absolute calibration leads to an error of about 10% in determining the mesospheric CO₂ volume mixing ratio [17].

The CO₂ volume mixing ratios are determined from the retrieved profiles of the temperature, pressure, and CO₂ number concentration. Therefore, the possibilities of the improved combined method of interpreting the CRISTA data for determination of the CO₂ volume mixing ratio profiles can be best demonstrated by numerical experiments. Figure 1 presents examples of numerical experiments. As “actual” profiles of the CO₂ volume mixing ratio, we used profiles having constant volume mixing ratios up to different heights and having different gradients above these heights. All retrieved profiles presented in Fig. 1 coincide, within the computational errors, with the corresponding “actual” profiles over a wide height range (in these numerical experiments, the random error of retrieval was solely taken into account). About the point of inflection, the

Table 2. Errors in CO₂ volume mixing ratio retrieval

Height	Random component		Systematic component	
	ppmv ⁻¹	%	ppmv ⁻¹	%
60	6	2	6	2
65	8	2	12	3
70	11	3	1	1
75	9	3	2	1
80	10	4	21	7
85	13	5	43	17
90	17	8	53	25

retrieved and actual profiles agree to within twice the error. Note that, in spite of significant a priori limitations on the smoothness of the profile (a model correlation matrix characterized by the 20-km correlation distance was used for the volume mixing ratio profile), the height at which the volume mixing ratio begins to decrease is determined in numerical experiments with an error of 2.5 km, equal to the mesh width of the height grid. The CO₂ number concentration and thus the volume mixing ratio are the parameters of the inverse problem for which there are the least data because of physical causes first—the radiation absorption is small at the heights of interest. Therefore, we did not aim at determining small-scale variations in the CO₂ volume mixing ratio profile but sought the solution as a smooth function by introducing the corresponding a priori information. Finally, we also note that the systematic

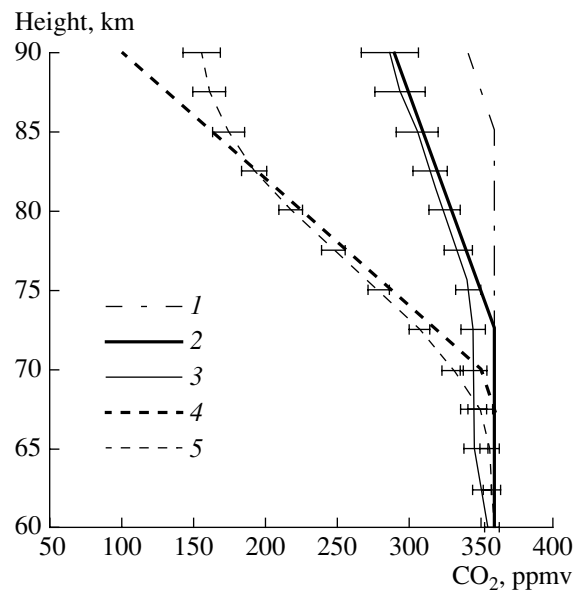


Fig. 1. Retrieved profiles of the CO₂ volume mixing ratio in numerical experiments: (1) a priori profile; (2), (4) “actual” profiles; and (3), (5) retrieved profiles (the bars correspond to the random component of the retrieval error).

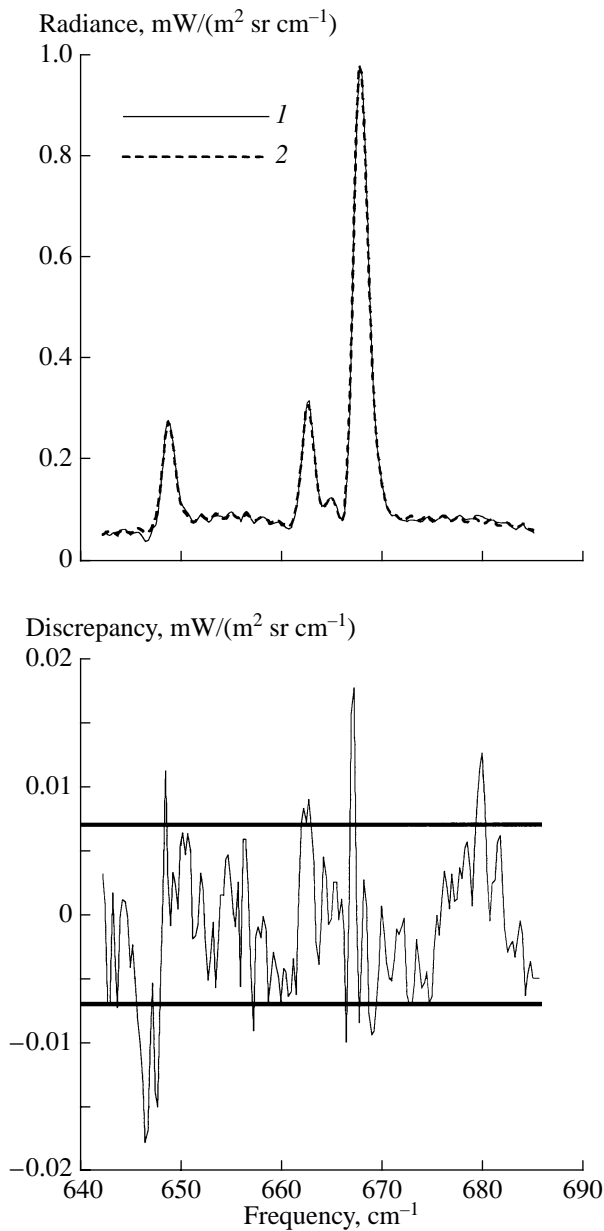


Fig. 2. Upper plot: an example of comparison of the radiances (1) measured and (2) computed by using the retrieved profiles of the atmospheric parameters. Lower plot: the corresponding spectral discrepancy (difference between the measured and computed radiances); the belt between straight lines characterizes the measurement error. The tangent height is 86.7 km; scan 1301.

error is comparable with the random error up to a height of about 80 km, and, therefore, when processing real data for heights not exceeding 80 km, we compute the height at which the volume mixing ratio begins to decrease with an error of 5 km.

The quality of the results can be assessed from the values of the spectral residual, i.e., from the discrepancy between the radiances measured and those com-

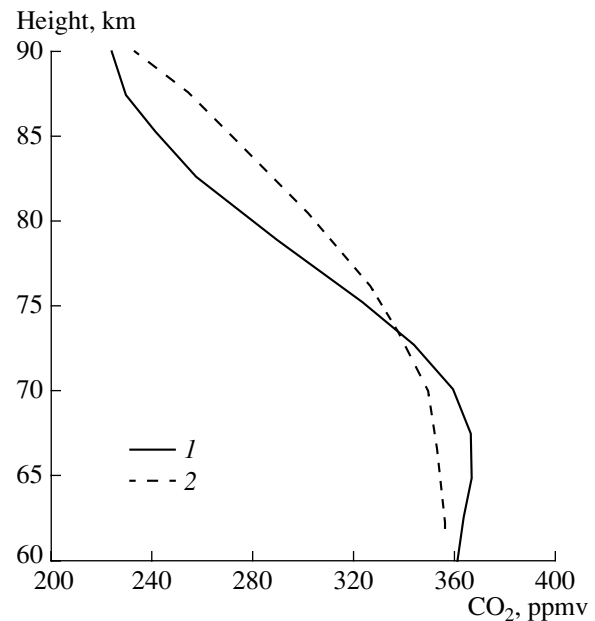


Fig. 3. Comparison of the mean CO₂ volume mixing ratio profiles obtained (1) in this work and (2) by an independent method from the CRISTA-1 data.

puted from the retrieved profiles of atmospheric parameters. An example is given in Fig. 2, where the results relevant to one of the scans corresponding to a tangent height of 86.7 km are presented. It is seen that the computed spectrum reproduces the measured values with a high accuracy. At this tangent height, the total error of measurements is approximated by a value of 0.007 mW/(m² sr cm⁻¹). The presented data show that the discrepancy throughout almost the entire spectral range is within “the corridor of errors.”

An indirect confirmation of the quality of the information on the mesospheric CO₂ content presented in our work is Fig. 3, where the CO₂ volume mixing ratio mean profiles obtained in [10] and in this work are presented. It is necessary to take into account that the profile in [10] represents the full data file on the outgoing radiation measured in the daytime only in the course of the CRISTA-1 experiment and the profile presented by us is obtained on the basis of a limited sampling containing 272 scans measured under daytime and nighttime conditions. From Fig. 3, it follows that the two profiles coincide in the limits of measurement errors. Taking into account that the information on the CO₂ content is retrieved by the authors of these two works from measurements of emission in different CO₂ bands (4.3- and 15- μ m bands in [10] and in our work, respectively) and that the physical principles of the CO₂ content indirect measurements are radically different, the comparison presented in Fig. 3 can be regarded as validation of two independent measurements.

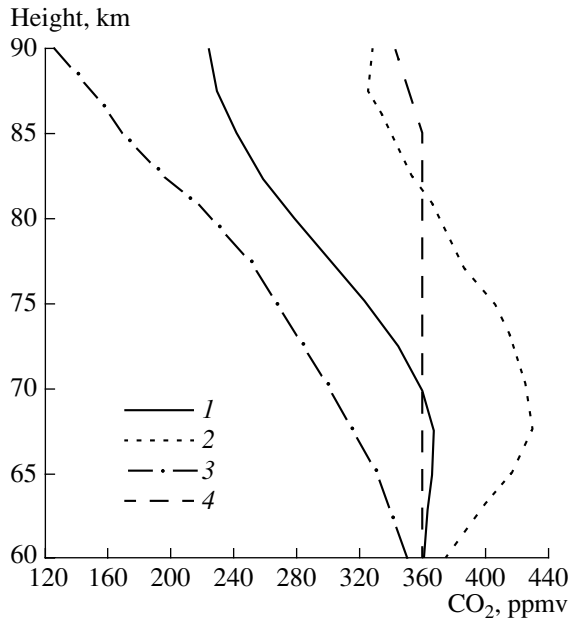


Fig. 4. (1) the mean CO₂ volume mixing ratio profile obtained on the basis of all processed scans; (2) and (3) the boundaries of the range of retrieved parameters; and (4) the a priori profile used to solve the inverse problem.

3. RESULTS OF INTERPRETATION OF THE CRISTA-1 DATA

Figure 3, where the CO₂ volume mixing ratio mean profiles obtained by us and by the authors of [10] (below, these profiles are denoted as 1 and 2, respectively) are compared, demonstrates a good correlation between two independent measurements and the following peculiarities.

(1) The fall of the CO₂ volume mixing ratio in both mean profiles begins at nearly the same height, about 70 km.

(2) In the height range 70–80 km, the rates of the CO₂ volume mixing ratio fall with increasing height differ significantly in profiles 1 and 2. The height gradient for profile 1 is noticeably higher than that for profile 2.

(3) In the height range 60–70 km, the CO₂ volume mixing ratios in profile 1 exceed those in profile 2. The maximum difference ranges up to 18 ppmv, i.e., up to about 5%. Above 74 km, profile 1 is characterized by lower volume mixing ratios than profile 2. The differences reach 22 ppmv, i.e., about 10%. At a height of 90 km, the volume mixing ratios obtained from two independent measurements practically coincide.

Figure 4 presents the CO₂ volume mixing ratio profile taken from [21] and used as an a priori profile in solving the inverse problem, the average profile obtained from our measurements, and two curves enveloping the maximum and minimum volume mixing ratios obtained from the entire set of 272 scans. The

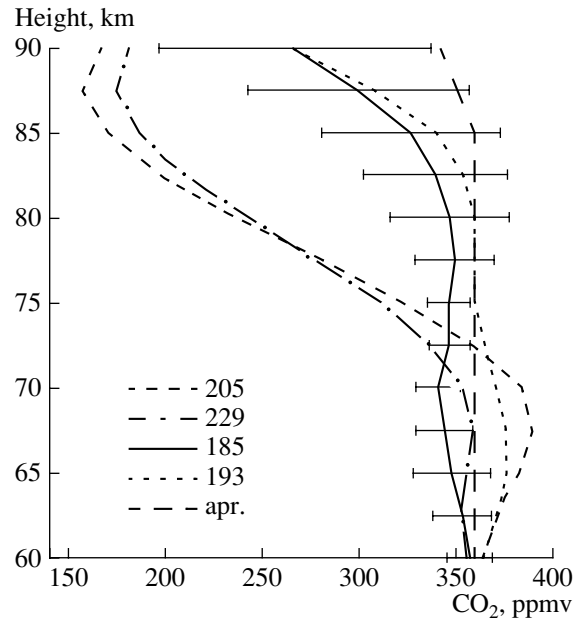


Fig. 5. CO₂ volume mixing ratio profiles characterized by minimum and maximum CO₂ volume mixing ratios retrieved for a height of 85 km. The numbers of the corresponding scans are indicated in the legend; “apr.” is the a priori profile used to solve the inverse problem. The retrieval errors are indicated for one of the profiles.

spread in the volume mixing ratio values is significant and involves both measurement errors and natural variations in the CO₂ content. The CO₂ volume mixing ratios retrieved repeatedly by us for the height range 60–75 km noticeably exceed the model value of 360 ppmv. The deviations from this model value reach 60 ppmv. If CO₂ is uniformly mixed over this height range and the deviations from the model profile are caused by random and systematic measurement errors, this spread in values allows indirect estimation of the error of our measurements performed at these heights (natural variations in the volume mixing ratio should not be completely ruled out over this height range). Equating the value 60 ppmv to three standard deviations, we conclude that the rms measurement errors in the volume mixing ratio at these heights is equal to 20 ppmv, i.e., 5.5%. We note that this indirect estimate of the retrieval errors agrees well with their independent estimates presented in Section 2.

An analysis of individual retrievals shows that the total set of the CO₂ volume mixing ratio profiles includes profiles of two types. Figure 5 presents the CO₂ volume mixing ratio profiles demonstrating a rapid fall beginning at a height of 70 km and those demonstrating a nearly constant volume mixing ratio up to a height of about 85 km. The occurrence of profiles with the principal differences far exceeding the retrieval errors for individual profiles indicates that significant variations in the volume mixing ratio are characteristic of atmospheric heights above 75 km. Moreover, Fig. 5

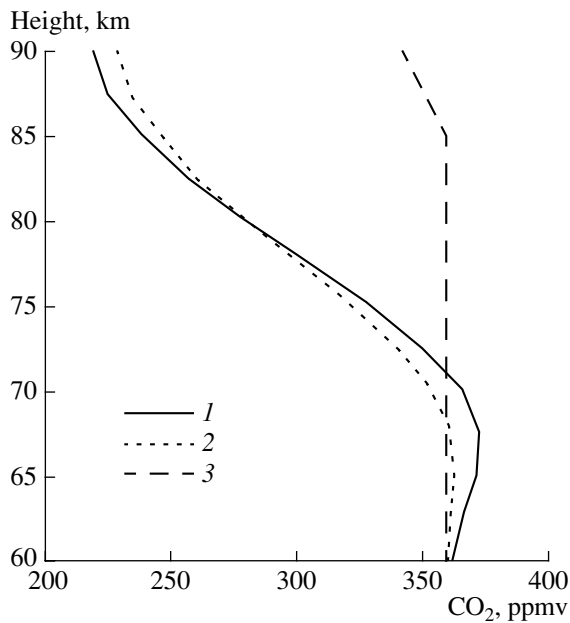


Fig. 6. Mean CO₂ volume mixing ratio profiles computed from (1) daytime and (2) nighttime measurements; (3) the a priori profile used to solve the inverse problem.

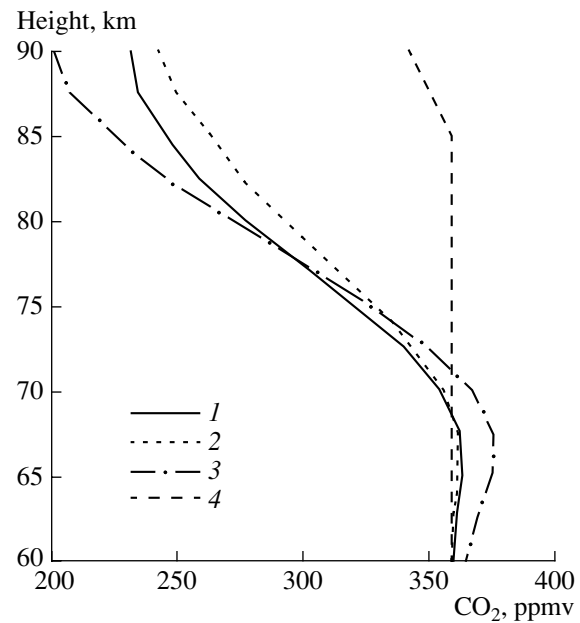


Fig. 7. Mean CO₂ volume mixing ratio profiles computed for the latitude belts (1) 30° S–30° N, (2) to the south of 30° S, and (3) to the north of 30° N; (4) the a priori profile used to solve the inverse problem.

can partially explain the contradiction occurring between the data on the height of the beginning of CO₂ volume mixing ratio fall revealed in a number of measurements performed independently in different times and geographic points. These data are briefly analyzed in the introduction. According to Fig. 5, the differences between the volume mixing ratios constituting the profiles of two types reach 160 ppmv. We emphasize that, among 272 CO₂ volume mixing ratio profiles retrieved by us, only six realizations are nearly constant up to a height of 85 km (the volume mixing ratio exceeds 300 ppmv at a height of 85 km).

Note that, due to a significant systematic error (20–30% at heights of 85 to 90 km), our retrieval procedure does not reveal statistically significant natural variations in the mesospheric CO₂. This conclusion is confirmed in [16], where it is indicated that latitudinal and seasonal variations in the CO₂ volume mixing ratio do not exceed 10% at a height of 85 km and 14% at a height of 90 km. Nevertheless, individual retrievals testify to significant variations in the CO₂ content in the upper mesosphere at heights of 80 to 90 km (see Fig. 5).

Figure 6 presents the mean profiles of the CO₂ volume mixing ratio for daytime and nighttime conditions. As a result of averaging, the random error in retrieving these profiles is rather small and, according to our estimations, is limited by 1%. The differences between the daytime and nighttime mean profiles are insignificant and do not exceed 10–12 ppmv. In the lower mesosphere (the height range 60–75 km), the daytime CO₂ volume mixing ratio values are higher than the nighttime values;

however, the opposite situation occurs at heights of 80 to 90 km. Note that the theoretical modeling of the atmospheric composition (see, for example, [6]) shows the occurrence of daily variations in the CO₂ density above 100 km. In the nighttime, the CO₂ density is higher and the diffusion equilibrium must be established at lower heights. This effect is seen in Fig. 6.

Spatial variations in the CO₂ volume mixing ratio can be observed from the data shown in Fig. 7, which presents the mean profiles for the equatorial region 30° S–30° N and for the middle latitudes 30°–60° of the Northern and Southern hemispheres. In the height range 85–90 km, the latitudinal differences in the CO₂ content reach 40 ppmv and can be regarded as statistically significant, because averaging largely suppresses the random error in retrieved values. Over this height range, the minimum and maximum volume mixing ratios are observed in the middle latitudes of the Northern (fall) and Southern (spring) hemispheres, respectively.

The analysis of the latitudinal dependences of the CO₂ volume mixing ratio and density can be continued with Figs. 8 and 9. Figure 8 presents the latitudinal functions of the mesospheric CO₂ volume mixing ratio retrieved for different heights and their linear approximations computed with the least-squares method. Although the data spread is significant for individual retrievals, the following peculiarities can be noted. As is seen from Fig. 8, no latitudinal variations in the volume mixing ratio at a height of 75 km occur. On the other hand, at heights of 80, 85, and 90 km, the ten-

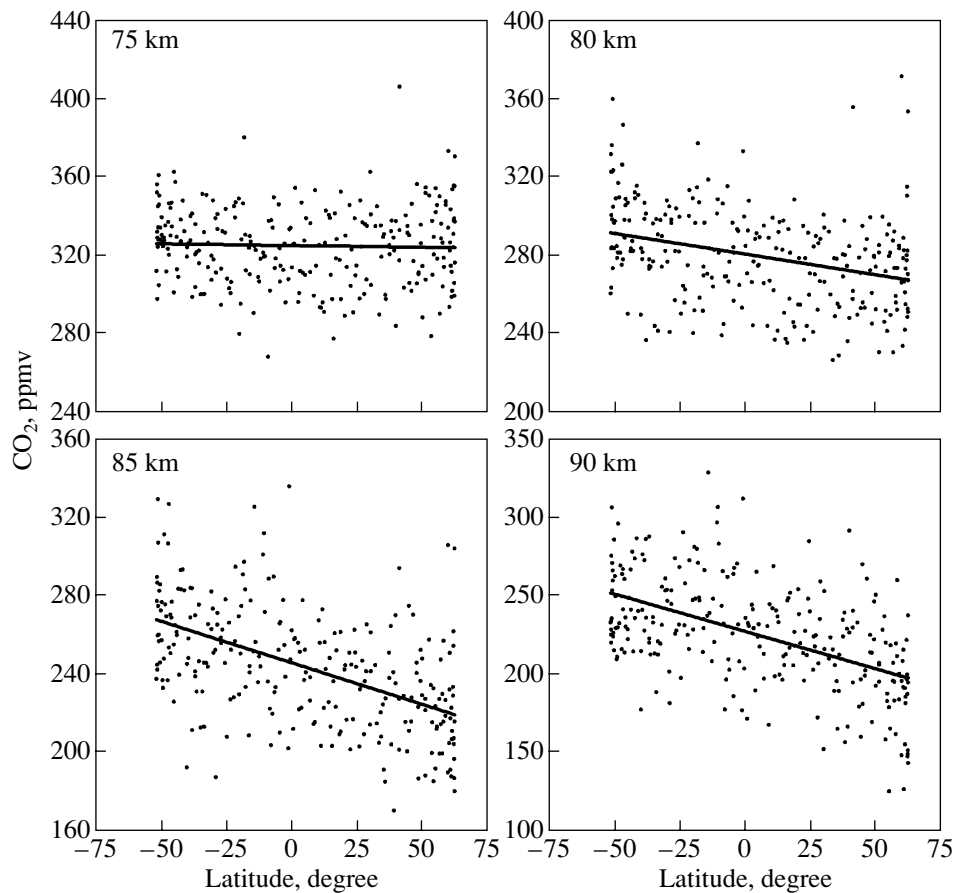


Fig. 8. Latitudinal distribution of the CO₂ volume mixing ratio retrieved for heights of 75, 80, 85, and 90 km. Solid lines represent a linear approximations of the latitudinal dependence.

dency of CO₂ volume mixing ratio decreasing in the direction from the south (spring) to the north (fall) is observed. The mean gradients of volume mixing ratio decreasing at heights of 80, 85, and 90 km are equal to 2.1, 4.2, and 4.8 ppmv per 10° of latitude, respectively. The mean volume mixing ratio differences occurring between latitudes of 50° S and 50° N are equal to 21, 42, and 48 ppmv for heights of 80, 85, and 90 km, respectively.

Figure 9 demonstrates analogous latitudinal variations in the mesospheric CO₂ densities retrieved for different heights. A northward height-dependent trend of CO₂ concentration decrease reveals itself in the height range from 75 to 90 km. The mean latitudinal gradients in the concentration are equal to 5.0×10^8 , 2.1×10^8 , 9.0×10^7 , and 2.5×10^7 cm⁻³ per 10° at heights of 75, 80, 85, and 90 km, respectively.

Above, the CO₂ volume mixing ratios retrieved from the CRISTA-1 data by experts from Wuppertal [10] and St. Petersburg (this work) universities are compared. This comparison demonstrates a very close agreement between two independent approaches to mesospheric CO₂ content retrieval. The most important difference lies in the values of the height gradients of volume mixing ratio decreasing. In a number of figures,

the results of our retrievals are compared with the model profile taken from [21] and used by us as an a priori profile in solving the inverse problem. Figure 10 combines the mean profile of the CO₂ volume mixing ratio retrieved by us and different profiles proposed by other authors.

A comparison between the profiles retrieved by us and the model profiles (curves 3, 4, 7) shows that significant differences occur between the heights at which the CO₂ volume mixing ratio begins to decrease. However, a satisfactory agreement between our results and the ATMOS experiment results obtained for heights up to 85 km is observed. Not only the previous results but also the results of [10] obtained with the modern numerical TIME-GCM model show that theoretical models predict the beginning of volume mixing ratio fall at heights significantly exceeding those observed in most of the experiments. This contradiction could be largely removed if the multiformity revealed by us in the volume mixing ratio profiles over the entire set of retrieved profiles would be taken into consideration (Fig. 4). However, for the majority of retrievals and also for the averaged data (Fig. 3), the experimental results indicate that the numerical atmospheric models are inadequate for the description of the height below which CO₂ is uniformly mixed.

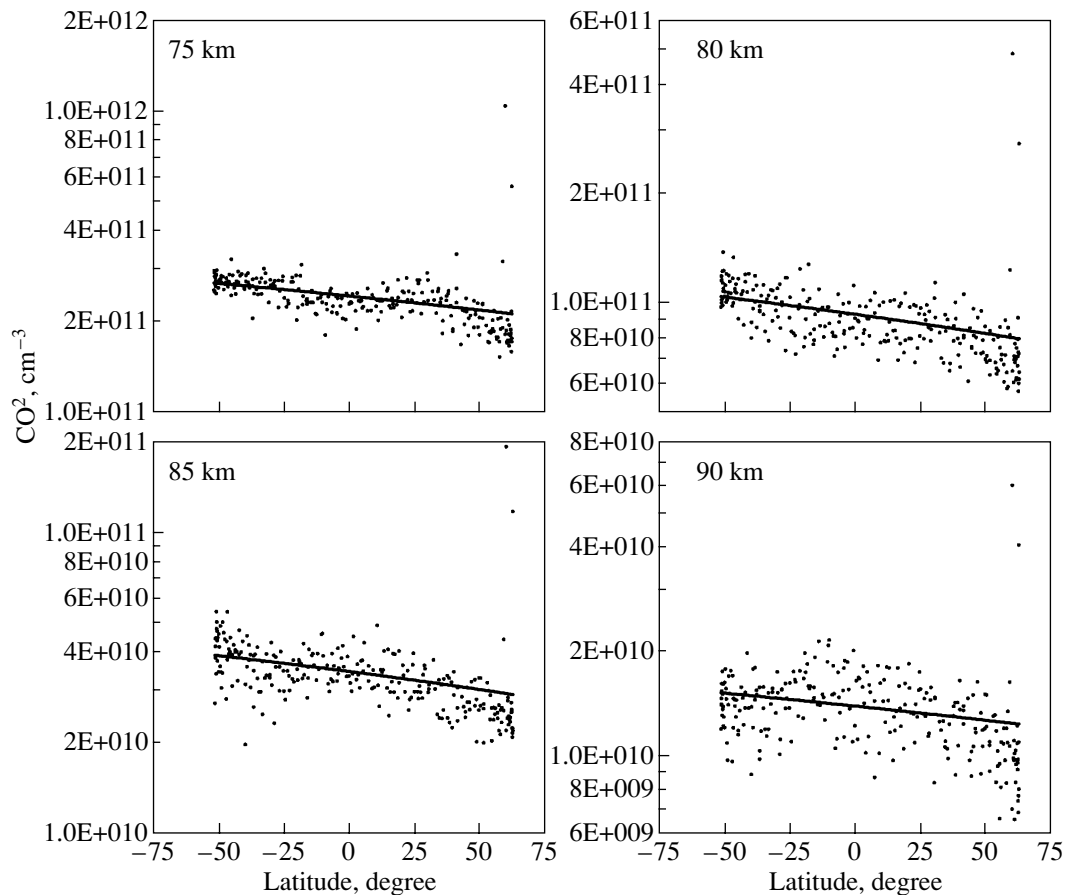


Fig. 9. Latitudinal distribution of the CO₂ concentration retrieved for heights of 75, 80, 85, and 90 km. Solid lines represent linear approximations of the latitudinal dependence.

4. PRINCIPAL RESULTS AND CONCLUSIONS

The current state of the problem of mesospheric CO₂ content investigation is analyzed. It is shown that the modern experimental data and numerical simulations lead to different heights at which the CO₂ volume mixing ratio begins to fall, i.e., the heights below which CO₂ is uniformly mixed. The height gradients of the volume mixing ratio are different in the layer from 70 to 100 km.

An algorithm of retrieving the CO₂ concentration and volume mixing ratio from the Earth's limb outgoing radiance measured with the CRISTA satellite instrument in the CO₂ 15- μ m band is described. An analysis of retrieval errors is given.

The mesospheric CO₂ content profiles obtained for the height range 60–90 km as a result of interpretation of 272 scans of the Earth's limb outgoing radiation measured in November 1994 with the CRISTA satellite instrument in the CO₂ 15- μ m band over the latitude belt 55° S–65° N are presented and analyzed.

Below, the principal conclusions of this work are briefly formulated.

(1) The errors in retrieving individual volume mixing ratio profiles is smaller than 10% for heights up to about 80 km and is 20 and 30% for heights of 85 and 95 km, respectively.

(2) Comparisons of the CO₂ contents retrieved from the CRISTA-1 data independently at St. Petersburg State University and Wuppertal University [10] demonstrate a good general agreement of the mean profiles. In most independent retrievals based on different CO₂ absorption bands and different physical principles of remote measurements, the CO₂ volume mixing ratio begins to decrease at a height of 70 to 75 km in cases. This agreement is an indirect validation of the quality of the data obtained by different methods. However, for the mean profiles under comparison, the CO₂ volume mixing ratios decrease with significantly different rates at heights of 70 to 80 km.

(3) The spread in the retrieved values of the CO₂ volume mixing ratio is significant and includes both the measurement errors and natural CO₂ content variations. Differentiation of these spread components is now difficult. However, our results indicate without doubt that the entire set contains retrieved profiles of two types demonstrating different behaviors of the CO₂ volume mixing

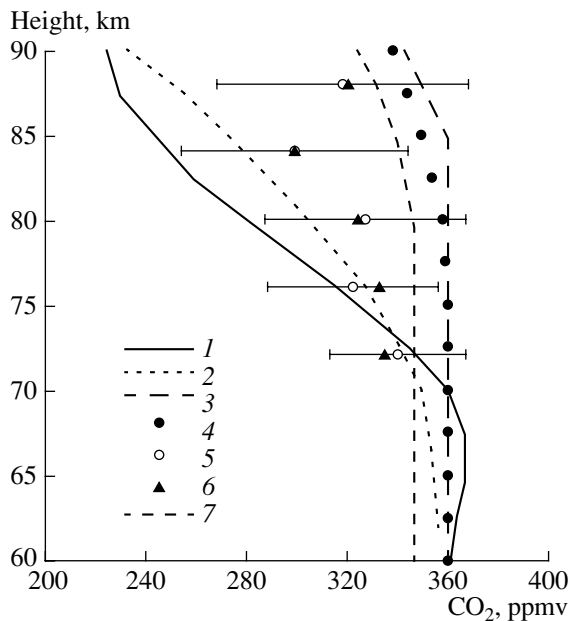


Fig. 10. Intercomparison of the CO₂ volume mixing ratio mean profiles computed or used as a model in the following works: (1) this work; (2) [10], Fig. 13, independent method, the CRISTA-1 experiment; (3) [21], model; (4) AFGL-86 model, the range of complete mixing, scaling to a value of 360 ppmv; (5) and (6) [13], the ATMOS experiment; and (7) [22], model.

ratio: a rapid increase beginning at a height of 70 km and near-constancy up to a height of about 85 km; the later type is rare in occurrence. These results partially explain the discrepancy between the data of independent measurements (performed at different times and geographic sites) of the atmospheric heights at which the CO₂ volume mixing ratio begins to decrease. Our results are also indicative of the variability of the processes of mixing and diffusion equilibrium in the Earth's atmosphere over the height range 70–90 km.

(4) Our analysis of the daytime and nighttime mean profiles of the CO₂ volume mixing ratio reveals no significant daily variations in the CO₂ content. However, taking into account that data averaging significantly reduces the random retrieval errors, we can note that the differences between the daytime and nighttime mean profiles reach 10–12 ppmv. The daytime volume mixing ratios exceed their nighttime values in the lower mesosphere (60–75 km), and the opposite situation is observed in the height range 80–90 km.

(5) The latitudinal dependences of the CO₂ volume mixing ratio and concentration are obtained. These characteristics demonstrate a CO₂ decrease in the northward direction. Note that the reverse latitudinal dependence is observed in [10] for the CO₂ density at a height of 85 km, namely, the CO₂ density increases toward northern latitudes. However, this result is obtained in [10] for the CRISTA-2 experiment. Recall

that the CRISTA-2 experiment was performed in the period August 8–16, 1997, and the CRISTA-1 experiment, the results of which are presented in this work, was performed in the period November 4–12, 1994. It is possible that the revealed differences demonstrate seasonal or interannual variations in the CO₂ content at these heights.

(6) A comparison of the retrieved profiles with the model profiles indicates that significant differences between the atmospheric heights at which the CO₂ volume mixing ratio begins to decrease are observed. For the majority of retrievals (as for the mean data), experimental results indicate that the numerical atmospheric models are inadequate for the description of the height of CO₂ uniform mixing.

ACKNOWLEDGMENTS

We are grateful to our colleagues from the University of Wuppertal for putting the CRISTA-1 data at our disposal and for useful discussions.

This work was supported by the Russian Foundation for Basic Research (project no. 00-05-65223) and the Russian Ministry of Education under the aegis of the Russian Universities Program (project no. 015.01.01.085).

REFERENCES

1. Seinfeld, J.H. and Pandis, S.N., *Atmospheric Chemistry and Physics, From Air Pollution to Climate Change*, Wiley, 1998, p. 1326.
2. Golitsin, G.S. *et al.*, Long-Term Temperature Trends in the Middle and Upper Atmosphere, *Geophys. Res. Lett.*, 1996, vol. 23, no. 14, pp. 1741–1744.
3. Offermann, D. and Grossmann, K.U., Thermospheric Density and Composition As Determined by a Mass Spectrometer with Cryo Ion Source, *J. Geophys. Res.*, 1973, vol. 78, no. 5, pp. 8296–8304.
4. Philbrick, C.R., Faucher, G.A., and Trzcinski, E., Rocket Measurements of Mesospheric and Lower Thermospheric Composition, *Space Res., Akad. Berlin*, 1973, vol. 13, pp. 255–260.
5. Offermann, D. *et al.*, Neutral Gas Composition Measurements between 80–120 km, *Planet. Space Sci.*, 1981, vol. 29, no. 4, pp. 747–764.
6. Trinks, H. and Fricke, K.H., Carbon Dioxide Concentration in the Lower Thermosphere, *J. Geophys. Res. D*, 1978, vol. 83, no. 12, pp. 3883–3886.
7. Hays, P.B. and Oliver, J.J., Carbon Dioxide and Monoxide above the Troposphere, *Planet. Space Sci.*, 1970, vol. 18, no. 10, pp. 1729–1733.
8. Wofsy, S.C., McConnell, J.C., and McElroy, M.B., Atmospheric CH₄, CO, and CO₂, *J. Geophys. Res. D*, 1972, vol. 77, no. 24, pp. 4477–4493.
9. Rodrigo, R. *et al.*, Neutral Atmospheric Composition between 60 and 220 km: A Theoretical Model for Mid-Latitudes, *Planet. Space Sci.*, 1986, vol. 34, no. 4, pp. 723–743.
10. Kaufmann, M. *et al.*, The Vertical and Horizontal Distribution of CO₂ Densities in the Upper Mesosphere and

- Lower Thermosphere As Measured by CRISTA, *J. Geophys. Res. D*, 2002, vol. 107, no. 23.
11. Timofeyev, Yu.M., Satellite Methods of Studying the Gas Composition of the Atmosphere (Review), *Izv. Akad. Nauk SSSR, Fiz. Atmos. Okeana*, 1989, vol. 26, no. 5, pp. 451–472.
 12. Girard, A. *et al.*, Global Results of GRILLE Spectrometer Experiment on Board Spacelab 1, *Planet. Space Sci.*, 1988, vol. 36, no. 2, pp. 291–300.
 13. Rinsland, C. *et al.*, Middle and Upper Atmosphere Pressure-Temperature Profiles and the Abundance of CO₂ and CO in the Upper Atmosphere from ATMOS/Spacelab 3 Observations, *J. Geophys. Res. D*, 1992, vol. 97, no. 18, pp. 20479–20295.
 14. Wintersteiner, P.P. *et al.*, Line-by-Line Radiative Excitation Model for the Nonequilibrium Atmosphere: Application to CO₂ 15 μm Emission, *J. Geophys. Res. D*, 1992, vol. 97, no. 16, pp. 18083–18117.
 15. Lopez-Puertas, M. and Taylor, F.W., Carbon Dioxide 4.3-μm Emission in the Earth's Atmosphere: A Comparison between Nimbus 7 SAMS Measurements and Non-Local Thermodynamic Equilibrium Radiative Transfer Calculations, *J. Geophys. Res. D*, 1989, vol. 94, no. 10, pp. 13045–13068.
 16. Zaragoza, G., Lopez-Puertas, M., Lopez-Valverde, M.A., and Taylor, F.W., Global Distribution of CO₂ in the Upper Mesosphere As Derived from UARS/ISAMS Measurements, *J. Geophys. Res. D*, 2000, vol. 105, no. 15, pp. 19829–19839.
 17. Kostsov, V.S. and Timofeyev, Yu.M., Interpretation of Satellite Measurements of the Outgoing Nonequilibrium IR Radiation in the CO₂ 15-μm Band: 1. Description of the Method and Analysis of Its Accuracy, *Izv. Akad. Nauk, Fiz. Atmos. Okeana*, 2001, vol. 37, no. 6, pp. 789–800 [*Izv., Atmos. Ocean. Phys.* (Engl. Transl.), vol. 37, no. 6, pp. 728–738].
 18. Timofeyev, Yu.M., Satellite IR Sounding of the Non-LTE Middle Atmosphere, *Proc. Int. Radiation Symp. IRS-2000: Current Problems in Atmospheric Radiation*, Smith, W. and Timofeyev, Yu., Eds., Deepak, 2001, pp. 757–760.
 19. Kostsov, V.S., Timofeyev, Yu.M., Grossmann, K., Kaufmann, M., and Oberkhaide, I., Interpretation of Satellite Measurements of the Outgoing Nonequilibrium IR Radiation in the CO₂ 15-μm Band: 2. Processing the CRISTA Experimental Data, *Izv. Akad. Nauk, Fiz. Atmos. Okeana*, 2001, vol. 37, no. 6, pp. 801–810 [*Izv., Atmos. Ocean. Phys.* (Engl. Transl.), vol. 37, no. 6, pp. 739–747].
 20. Clarmann, T.V., Linden, A., Funke, B., Dudhia, A., Edwards, D.P., Lopez-Puertas, M., Kerridge, B., Kostsov, V., and Timofeyev, Yu., Intercomparison of Non-LTE Radiative Transfer Codes, *Proc. Int. Radiation Symp. IRS-2000: Current Problems in Atmospheric Radiation*, Smith, W. and Timofeyev, Yu., Eds., Deepak, 2001, pp. 765–768.
 21. Shved, G.M., Kutepov, A.A., and Ogibalov, V.P., Non-Local Thermodynamic Equilibrium in CO₂ in the Middle Atmosphere. I. Input Data and Populations of the ν₃ Mode Manifold States, *J. Atmos. Solar-Terr. Phys.*, 1998, vol. 60, no. 3, pp. 289–314.
 22. Stiller, G.P. *et al.*, Stratospheric and Mesospheric Pressure-Temperature Profiles from Rotational Analysis of CO₂ Lines in Atmospheric Trace Molecule Spectroscopy/ATLAS 1 Infrared Solar Occultation Spectra, *J. Geophys. Res. D*, 1995, vol. 100, no. 2, pp. 3107–3117.

Translated by E. Kadyshovich